

## Research Article

# Estimating Deformation Modulus and Bearing Capacity of Deep Soils from Dynamic Penetration Test

Shihan Shan,<sup>1,2</sup> Xiangjun Pei,<sup>1</sup> and Weiwei Zhan <sup>1</sup>

<sup>1</sup>State Key Laboratory of Geohazard Prevention and Geoenvironment Protection, Chengdu University of Technology, Chengdu 610059, China

<sup>2</sup>Power China Chengdu Engineering Corporation Limited., Chengdu 610072, China

Correspondence should be addressed to Weiwei Zhan; [weiwei.zhan@tufts.edu](mailto:weiwei.zhan@tufts.edu)

Received 26 April 2021; Accepted 2 July 2021; Published 15 July 2021

Academic Editor: Antonello Troncone

Copyright © 2021 Shihan Shan et al. This is an open access article distributed under the Creative Commons Attribution License, which permits unrestricted use, distribution, and reproduction in any medium, provided the original work is properly cited.

The dynamic penetration test (DPT) and the Menard pressuremeter test (PMT) have been widely used in geotechnical survey of deep soils for megadam foundations in western China. The DPT measures are not well utilized due to the lack of correction factors and of empirical relationships for deep soils. This study investigates the relationships between the corrected DPT blow counts ( $N'_{120}$ ), pressuremeter modulus ( $E_{PMT}$ ), limit pressure ( $p_L$ ), deformation modulus ( $E_0$ ), and bearing capacity ( $f_{ak}$ ) derived from the PMT results. Meanwhile, a nonlinear regression model is developed to predict the DPT correction factor ( $a$ ) based on the raw DPT blow counts ( $N_{120}$ ) and the rod length ( $L$ ) by integrating the available correction factors for shallow gravelly soils suggested by the code provisions and the deep soil data in this work. It is concluded that the proposed DPT correction factors match well with the code suggestions and the new compiled dataset, and the corrected DPT blow counts can be used to reasonably predict the engineering properties of deep sand and clay soils. Although the proposed correlations need to be tested among different soil types and regions, the results shed the light on in situ geotechnical tests and data utilization for deep and thick overburden.

## 1. Introduction

Many megadams have been constructed on the valleys in western China to utilize the hydropower resources. The dam foundations are usually placed on the deep and thick overburden soils, which demand engineering properties of deep soils that are deeper than 20 meters. It is expensive to obtain undisturbed soil samples from the deep subsurface for laboratory tests. In situ tests have been widely used to estimate the engineering properties of these deep soils. The challenges in the interpretation of in situ soil tests mainly come from two aspects: (1) the complex soil behavior is influenced by intrinsic soil properties and many environmental factors such as temperature, pressure, and water availability [1]; (2) the lack of control and choice of the boundary conditions in field tests [2]. With increasing numbers of construction projects involving deep soils, it is desirable to explore the applications of in situ tests for these deep soils.

The dynamic cone penetration test (DPT) is widely used in the geotechnical survey in river valleys consisting of deep and thick overburden soils because of its characteristics of easy operation, wide applicability to different soil types, and relative low cost. The test consists of repeatedly dropping a hammer weighing 1177 N (120 kg) from a height of 100 cm onto an anvil that is connected by 60 mm diameter drill rods to a solid cone tip with a diameter of 74 mm and a cone angle of 60° [3]. Each hammer drop has potential energy that is theoretically equivalent to 1177 J. The number of blows by the hammer needed for the cone to penetrate the 10 cm strata is the counted  $N$ -value ( $N_{120}$ ). The DPT has been widely applied in Chinese geotechnical practices for foundation design since 1970s [3]. Recently, the DPT has been successfully applied to assess liquefaction of gravelly soils [3, 4]. However, the empirical correlation between DPT measures and soil properties such as deformation modulus and bearing capacity is limited to shallow gravelly soils with depth less than 20 m especially from the Chengdu Plain [5] (see Appendix A).

There are many factors that could influence the energy transmitted from the impact of the hammer on the anvil to the rod string and cone and thus affect the value of the blow count of hammer-impact penetration tests [6]. Calibration chamber tests [7, 8] and in situ measurements [6] are usually conducted to evaluate the influential factors on penetration tests and standardization procedure. There are few studies about the influential factors on DPT blow count and its correction. The energy transfer ratio (ETR), defined as the ratio of the energy that passes through the rods to the theoretical potential energy, is the most direct measure of the energy loss within the penetration test system. Cao et al. [3] reported that the Chinese DPT has an average ETR of 89% according to 1,200 hammer energy measurements within the shallow gravelly soils for liquefaction assessment. Zuo and Zhao [9] conducted a series of physical model tests that penetrate the soils within a model box with incremental rod lengths (up to 83 m) and compute the correction factors as the blow count of any rod length to the blow count of 2 m long rod under the same soil condition. Their results suggest that the correction factors of DPT gradually decrease with the increase of rod length (correction factor is around 0.5 when rod length is 83 m), which is independent of soil type and overburden pressure. Li et al. [10] measured the stress distribution at several rod depths using a series of in situ DPT tests. Their results suggest that the maximum peak stress drops nonlinearly along the rod length (from the top and bottom) and the maximum peak stress drop ratio increases with the rod length. Based on numerical simulation results, they proposed empirical correlations to estimate the rod-length-dependent correction factors for DPT blow counts. Based on many engineering practices, the Chinese Code for Investigation of Geotechnical Engineering [11], hereinafter called Chinese Code, suggests that the correction factors for DPT blow counts are simultaneously affected by the raw DPT blow counts and the rod length. However, the DPT correction factors suggested by the Chinese Code are limited to rod length below 19 m and raw DPT blow count less than 40 (see Appendix B).

This study attempts to expand the DPT correction factors for deep soils and to use the corrected DPT blow counts to predict deformation modulus and bearing capacity of deep soils. For these purposes, a database consisting of 74 pairs of DPT and pressuremeter test (PMT) results is compiled from a geotechnical survey project for a dam designed on a deep overburden site in southwestern China. The geology and geotechnical conditions of the study site are described in Section 2, and the in situ tests and data processing are detailed in Section 3. The empirical relationships for estimating DPT correction factors and engineering properties of soil using DPT test results are shown in Section 4, and the last section draws the conclusions.

## 2. Geological and Geotechnical Conditions

The study area is a dam construction site located in southwestern China. A high-rise dam will be placed on the river valley that consisted of very deep and thick overburden. Many types of geological and geotechnical surveys (see Figure 1)

have been conducted at the project site to investigate the structure and properties of the underlying soils. According to borehole data, the maximum thickness of overburden sediments reaches 567 m at the middle point of the river valley (ZKm304 in Figures 1 and 2). The overburden thickness decreases from the middle to the two sides, which is consistent with the old U-shape valley topography. The bedrock in the study area mainly consists of Precambrian gray gneiss ( $Pt_{2-3}Nq^d$ ) and is exposed on the valley slopes. The deep overburden can be divided to four major layers from the bottom to the top (i.e., from oldest to newest in geological age):

Layer I (Pleistocene gravelly soil, see Figure 3(f)): it is located at the bottom of the old riverbed. Its burial depth ranges from 350 to 460 m according to borehole investigations at different site locations. The geological origin of this layer is glacial outwash deposits ( $Q_3^{f8l+gl}$ ).

Layer II (Pleistocene cobble soil, see Figure 3(e)): its burial depth ranges from 200 to 250 m. Its geological origin is alluvial and pluvial deposits ( $Q_3^{al+pI}$ ).

Layer III (Pleistocene sand and clay soil): its burial depth ranges from 6 to 12 m and thickness ranges from 200 to 250 m. It majorly consists of sand, sandy silt, and silty clay. The geological origin of Layer III is alluvial and lacustrine deposits ( $Q_3^{al+lI}$ ).

Layer IV (Holocene gravelly soil, see Figure 3(a)): this layer is the modern alluvial deposit ( $Q_4^{al}$ ).

The engineering properties of Layer III will be the focus of this work as this soil layer will be used as the foundation soil to support a high-rise dam. The Layer III is made up of the Pleistocene alluvium and lacustrine sediments. According to the soil characteristics explored by the boreholes, this layer is further divided into three sublayers, and the major soils within each sublayer are described as following (from the bottom to the top):

Sublayer III-1: it is located at the bottom of Layer III. This sublayer majorly consists of dark gray to brownish-yellow sand (see Figure 3(d)). The particle size distribution is shown in Figure 4. Its average density is  $1.78 \text{ g/cm}^3$  and average moisture content is about 4.8%. The void ratio is 0.515 and the specific gravity is 2.69. The liquid limit (LL) and plasticity index (PI) are 20.4 and 8.9, respectively. The soil gradation measures, uniformity coefficient (Cu), and coefficient of gradation (Cc) are 7.6 and 1.0, respectively. According to the Unified Soil Classification System (USCS) [12], the soil is classified as well-graded sand with clay, with the group symbol as SW-SC (see Table 1). The burial depth of this sublayer ranges from 70 to 95 m. The layer thickness has large variation along the transverse (cross river) direction, with thickness of 20 to 40 m at two sides and 150 to 170 m at the middle.

Sublayer III-2: it is located at the middle of Layer III. It majorly consists of dark-gray clay and silt (see Figure 3(c)). The burial depth of this sublayer ranges from 50 to 80 m. The thickness ranges from 5.2 to 24.2 m, with an average value of 16 m. The major soil type of this sublayer is clay, with average density of  $1.56 \text{ g/cm}^3$  and moisture content of 16.3%. The void ratio is 0.746, and the specific gravity is 2.72. The liquid limit and plasticity index are 37.3 and 16.6, respectively. According to USCS, this soil is classified as lean clay with the group symbol of CL (see Table 1).

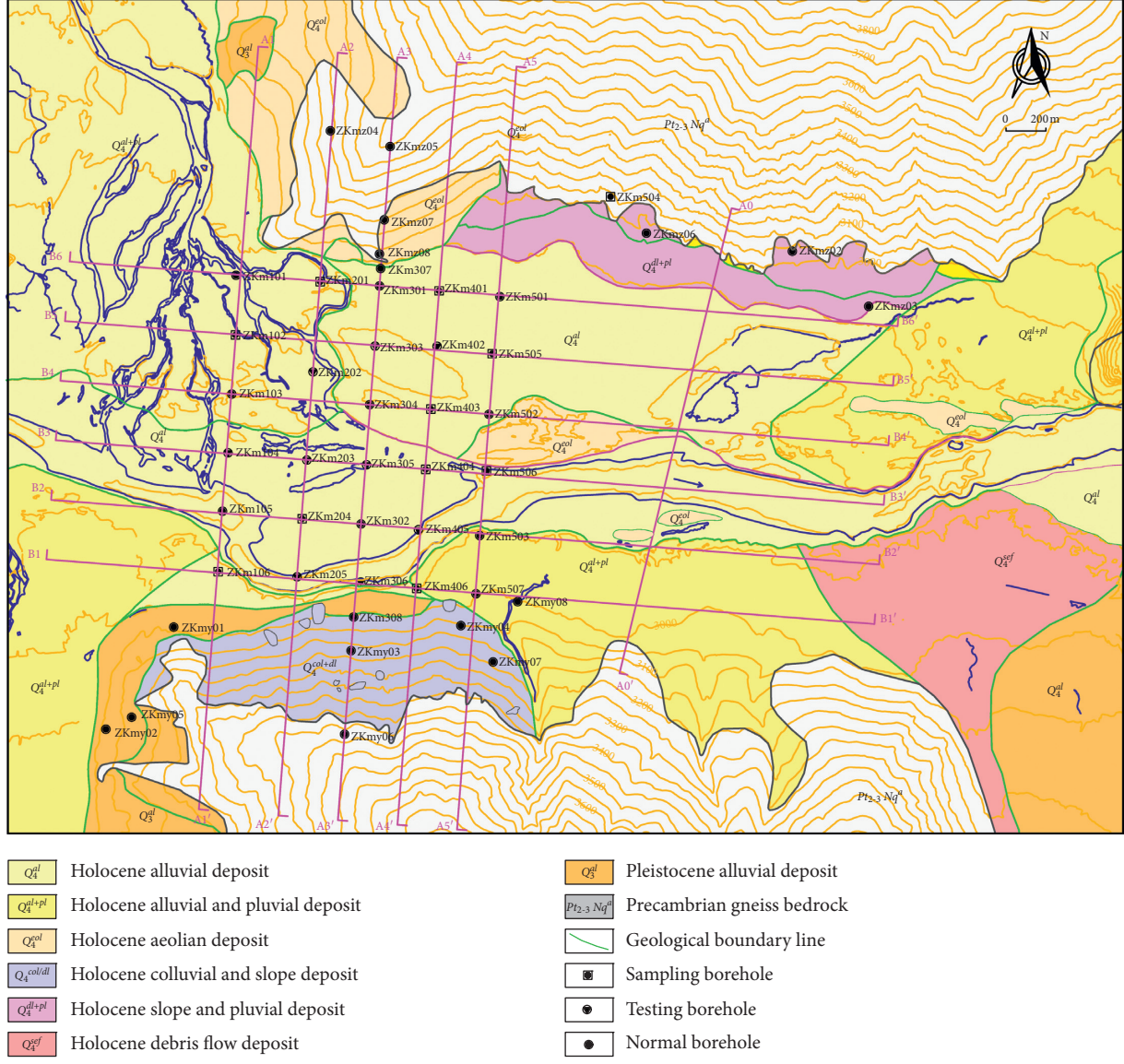


FIGURE 1: Site map showing locations of geotechnical investigations.

Sublayer III-3: it is located at the top of Layer III. It is made up of dark gray to brown sand (see Figure 3(b)). The burial depth ranges from 6 to 40 m. The thickness ranges from 36.85 to 53.8 m, with an average value of 46 m. The average density is 1.71 g/cm<sup>3</sup>, and the moisture content is 5.7%. The void ratio is 0.573, and the specific gravity is 2.68. The liquid limit and plasticity index are 19.3 and 8.5, respectively. The uniformity coefficient (Cu) and coefficient of gradation (Cc) are 6.6 and 1.1, respectively. According to USCS, the soil is classified as well-graded sand with clay, with the group symbol as SW-SC (see Table 1).

### 3. In Situ Tests and Data Processing

This study uses the dynamic cone penetration test (DPT) and pressuremeter test (PMT) results to develop regression models for estimating DPT correction factors and

engineering properties of soils (pressuremeter modulus, limit pressure, deformation modulus, and bearing capacity) within Layer III (burial depth ranges from 6 to 40 m). In total, 74 sets of data are collected from the nine boreholes shown in Table 2. According to Table 2, there are 10, 15, and 49 pairs of data for soils within sublayers III-1, III-2, and III-3, respectively. The 11 pairs of data among the 49 ones within the III-3 layer have rod length less than 19 m where the correction factors in the Chinese Code (see Appendix B) can be applied. The remaining 63 DPT measures will require new correction factors that are not available in the Chinese Code. The testing procedure and data processing methods for the DPT and PMT are briefly described in the following sections.

**3.1. Dynamic Penetration Test.** The dynamic penetration test (DPT) was developed in China during the early 1950s to measure the penetration resistance of gravelly soils.

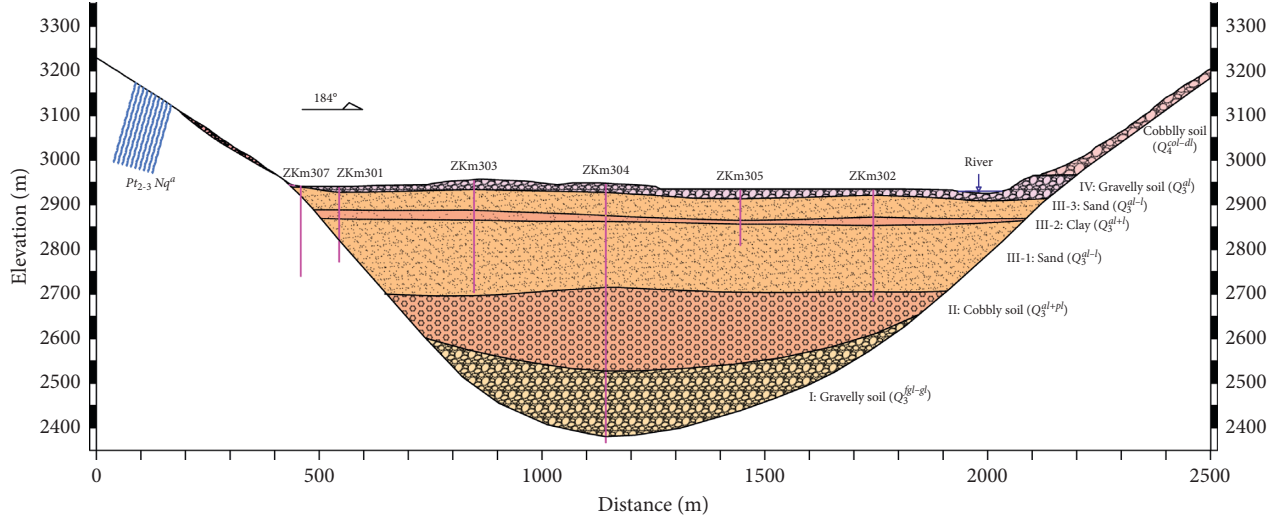


FIGURE 2: Soil profile map along the line A3-A3' in Figure 1.



FIGURE 3: Typical soil samples of different soil layers and depth (from ZKm304). (a) Layer IV. (b) Layer III-3. (c) Layer III-2. (d) Layer III-1. (e) Layer II. (f) Layer I.

DPT could provide an important new procedure for characterization of gravels and fill a gap in present geotechnical practice between CPT/SPT and BPT testing [4].

The DPT has been widely applied in Chinese geotechnical practices since the code provisions providing guidance for the foundation design using DPT were published in the

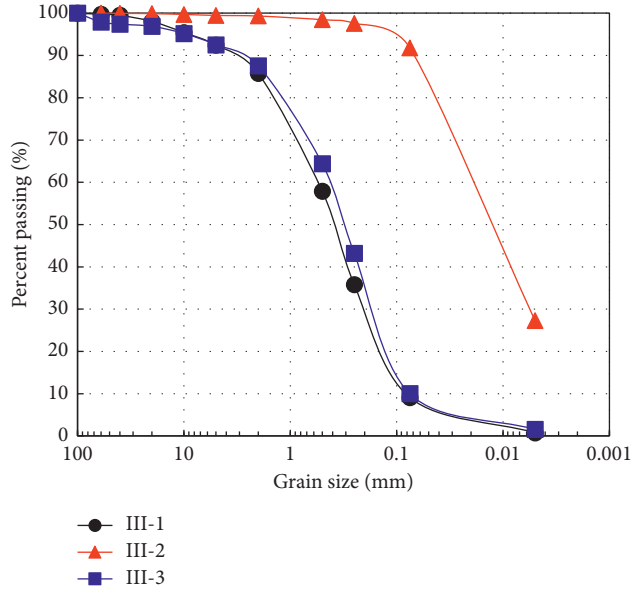


FIGURE 4: Averaged grain size distribution curves of soil samples from soil Layer III.

TABLE 1: Averaged soil parameters for soils within each sublayer of Layer III.

| Sublayer ID | USCS  | Group name                 | Density (g/cm <sup>3</sup> ) | Moisture content (%) | LL   | PI   | Cu  | Cc   |
|-------------|-------|----------------------------|------------------------------|----------------------|------|------|-----|------|
| III-3       | SW-SC | Well-graded sand with clay | 1.71                         | 5.7                  | 19.3 | 8.5  | 6.7 | 1.1  |
| III-2       | CL    | Lean clay                  | 1.56                         | 16.3                 | 37.3 | 16.6 | 10  | 0.64 |
| III-1       | SW-SC | Well-graded sand with clay | 1.78                         | 4.8                  | 20.4 | 8.9  | 7.6 | 1.0  |

TABLE 2: The database consisting of DPT, PMT measures, and engineering parameters.

| Borehole | ID | Soil layer | L (m) | N <sub>120</sub> | E <sub>PMT</sub> (MPa) | p <sub>0</sub> (kPa) | p <sub>f</sub> (kPa) | p <sub>L</sub> (kPa) | E <sub>0</sub> (MPa) | f <sub>ak</sub> (kPa) |
|----------|----|------------|-------|------------------|------------------------|----------------------|----------------------|----------------------|----------------------|-----------------------|
| ZKm102   | 1  | III-3      | 35.2  | 16               | 7.73                   | 230                  | 740                  | 1240                 | 30.98                | 510                   |
| ZKm102   | 2  | III-3      | 48.8  | 36               | 8.95                   | 270                  | 900                  | 1750                 | 46.47                | 630                   |
| ZKm102   | 3  | III-3      | 50.1  | 15               | 6.18                   | 270                  | 740                  | 1160                 | 27.57                | 470                   |
| ZKm102   | 4  | III-3      | 58.2  | 27               | 16.47                  | 360                  | 1000                 | 1480                 | 37.27                | 640                   |
| ZKm102   | 5  | III-2      | 68.2  | 11               | 4.21                   | 210                  | 550                  | 920                  | 22.21                | 340                   |
| ZKm102   | 6  | III-2      | 77.5  | 8                | 3.04                   | 200                  | 500                  | 800                  | 19.46                | 300                   |
| ZKm102   | 7  | III-1      | 82.5  | 43               | 9.75                   | 300                  | 1070                 | 1820                 | 47.75                | 770                   |
| ZKm102   | 8  | III-1      | 84.1  | 52               | 14.93                  | 450                  | 1100                 | 2080                 | 54.13                | 650                   |
| ZKm102   | 9  | III-1      | 93.5  | 47               | 11.03                  | 240                  | 1000                 | 1840                 | 49.39                | 760                   |
| ZKm102   | 10 | III-1      | 95.2  | 32               | 13.2                   | 260                  | 860                  | 1480                 | 37.92                | 600                   |
| ZKm106   | 11 | III-3      | 48.2  | 35               | 6.77                   | 180                  | 720                  | 1600                 | 46.31                | 540                   |
| ZKm106   | 12 | III-3      | 50.1  | 16               | 5.93                   | 220                  | 700                  | 1140                 | 28.34                | 480                   |
| ZKm106   | 13 | III-3      | 52.5  | 33               | 11.77                  | 240                  | 920                  | 1720                 | 43.91                | 680                   |
| ZKm106   | 14 | III-2      | 80.5  | 16               | 3.98                   | 190                  | 600                  | 1000                 | 26.18                | 410                   |
| ZKm106   | 15 | III-2      | 82.4  | 24               | 4.45                   | 180                  | 640                  | 1180                 | 33.1                 | 460                   |
| ZKm204   | 16 | III-3      | 22.4  | 10               | 5.34                   | 65                   | 510                  | 940                  | 26.87                | 445                   |
| ZKm204   | 17 | III-3      | 26.7  | 27               | 13.8                   | 120                  | 800                  | 1600                 | 44.03                | 680                   |
| ZKm204   | 18 | III-3      | 38.5  | 38               | 9.1                    | 140                  | 990                  | 1720                 | 50.68                | 850                   |
| ZKm204   | 19 | III-3      | 45.2  | 36               | 10.86                  | 150                  | 790                  | 1700                 | 47.58                | 640                   |
| ZKm204   | 20 | III-2      | 75.5  | 14               | 5.05                   | 65                   | 440                  | 850                  | 24.36                | 375                   |
| ZKm204   | 21 | III-2      | 78.2  | 15               | 5.24                   | 60                   | 490                  | 880                  | 25.33                | 430                   |
| ZKm401   | 22 | III-3      | 30.1  | 27               | 11.51                  | 140                  | 940                  | 1560                 | 42.76                | 800                   |
| ZKm401   | 23 | III-3      | 48.8  | 35               | 9.24                   | 200                  | 850                  | 1670                 | 46.19                | 650                   |
| ZKm401   | 24 | III-3      | 50.1  | 14               | 6.04                   | 270                  | 740                  | 1140                 | 26.9                 | 470                   |
| ZKm403   | 25 | III-3      | 21.8  | 15               | 8.47                   | 240                  | 800                  | 1330                 | 32.51                | 560                   |
| ZKm403   | 26 | III-3      | 23.2  | 18               | 11.53                  | 250                  | 900                  | 1380                 | 35.34                | 650                   |
| ZKm403   | 27 | III-3      | 32.2  | 25               | 10.21                  | 200                  | 920                  | 1550                 | 40.27                | 720                   |
| ZKm403   | 28 | III-3      | 34    | 22               | 10.67                  | 210                  | 900                  | 1420                 | 37.03                | 690                   |

TABLE 2: Continued.

| Borehole | ID | Soil layer | $L$ (m) | $N_{120}$ | $E_{PMT}$ (MPa) | $p_0$ (kPa) | $p_f$ (kPa) | $p_L$ (kPa) | $E_0$ (MPa) | $f_{ak}$ (kPa) |
|----------|----|------------|---------|-----------|-----------------|-------------|-------------|-------------|-------------|----------------|
| ZKm403   | 29 | III-3      | 45.5    | 33        | 11.2            | 280         | 870         | 1740        | 44.98       | 590            |
| ZKm403   | 30 | III-3      | 47      | 22        | 10.23           | 380         | 980         | 1560        | 35.06       | 600            |
| ZKm403   | 31 | III-3      | 60.2    | 26        | 15.63           | 320         | 880         | 1420        | 36.32       | 560            |
| ZKm403   | 32 | III-2      | 71.2    | 11        | 6.31            | 200         | 600         | 930         | 22.54       | 400            |
| ZKm403   | 33 | III-2      | 74.5    | 6         | 4.64            | 205         | 545         | 760         | 17.64       | 340            |
| ZKm403   | 34 | III-1      | 82.8    | 45        | 13.07           | 310         | 1070        | 1880        | 48.66       | 760            |
| ZKm403   | 35 | III-1      | 84.2    | 66        | 9.17            | 270         | 1010        | 2200        | 64.31       | 740            |
| ZKm404   | 36 | III-3      | 33.8    | 10        | 7.1             | 80          | 520         | 900         | 24.44       | 440            |
| ZKm404   | 37 | III-3      | 36      | 16        | 10              | 110         | 670         | 1090        | 30.54       | 560            |
| ZKm404   | 38 | III-3      | 48.8    | 23        | 9.63            | 230         | 810         | 1440        | 35.9        | 580            |
| ZKm404   | 39 | III-3      | 52      | 19        | 12.22           | 180         | 640         | 1140        | 31.55       | 460            |
| ZKm404   | 40 | III-2      | 64.5    | 4         | 4.65            | 110         | 420         | 600         | 15.43       | 310            |
| ZKm404   | 41 | III-2      | 67.2    | 7         | 3.94            | 130         | 410         | 730         | 18.88       | 280            |
| ZKm504   | 42 | III-3      | 40.63   | 36        | 6.34            | 320         | 1050        | 1740        | 48.42       | 730            |
| ZKm504   | 43 | III-3      | 42.1    | 42        | 8.08            | 320         | 1040        | 1950        | 53.64       | 720            |
| ZKm505   | 44 | III-3      | 25.5    | 11        | 6.88            | 110         | 520         | 1000        | 26.75       | 410            |
| ZKm505   | 45 | III-3      | 39.1    | 16        | 5.34            | 100         | 560         | 1020        | 29.61       | 460            |
| ZKm505   | 46 | III-3      | 40.83   | 26        | 10.31           | 250         | 940         | 1600        | 39.83       | 690            |
| ZKm505   | 47 | III-3      | 55.4    | 34        | 14.04           | 150         | 850         | 1620        | 43.84       | 700            |
| ZKm505   | 48 | III-2      | 63.8    | 10        | 3.79            | 260         | 650         | 960         | 22.05       | 390            |
| ZKm505   | 49 | III-2      | 65.2    | 9         | 3.76            | 100         | 440         | 760         | 20.82       | 340            |
| ZKm505   | 50 | III-2      | 70.1    | 17        | 4.75            | 110         | 520         | 1000        | 28.14       | 410            |
| ZKm505   | 51 | III-1      | 86.1    | 29        | 7.41            | 160         | 660         | 1320        | 36.64       | 500            |
| ZKm505   | 52 | III-1      | 89.7    | 51        | 13.23           | 180         | 1190        | 1900        | 52.88       | 1010           |
| ZKm506   | 53 | III-3      | 21.5    | 9         | 8.63            | 80          | 500         | 890         | 24.84       | 420            |
| ZKm506   | 54 | III-3      | 30.7    | 10        | 4.63            | 80          | 300         | 830         | 24.61       | 220            |
| ZKm506   | 55 | III-3      | 32.1    | 11        | 7.5             | 60          | 530         | 920         | 25.34       | 470            |
| ZKm506   | 56 | III-3      | 39.8    | 30        | 14.87           | 150         | 820         | 1570        | 43.77       | 670            |
| ZKm506   | 57 | III-3      | 55.8    | 18        | 4.39            | 70          | 480         | 990         | 29.98       | 410            |
| ZKm506   | 58 | III-2      | 68.2    | 14        | 6.95            | 60          | 430         | 920         | 25.64       | 370            |
| ZKm506   | 59 | III-2      | 70.1    | 10        | 4.66            | 60          | 380         | 720         | 20.9        | 320            |
| ZKm506   | 60 | III-1      | 79.8    | 51        | 10.91           | 140         | 920         | 1890        | 54.39       | 780            |
| ZKm506   | 61 | III-1      | 82.5    | 46        | 14.18           | 220         | 920         | 1820        | 49.89       | 700            |
| ZKm102   | 62 | III-3      | 12      | 20        | 17.42           | 300         | 1180        | 1480        | 39.98       | 420            |
| ZKm102   | 63 | III-3      | 15      | 10        | 8.51            | 200         | 630         | 1050        | 25.63       | 430            |
| ZKm204   | 64 | III-3      | 14.5    | 7         | 7.63            | 75          | 450         | 800         | 21.45       | 375            |
| ZKm204   | 65 | III-3      | 16.2    | 9         | 7.17            | 80          | 480         | 910         | 24.39       | 400            |
| ZKm204   | 66 | III-3      | 19.5    | 22        | 9.63            | 200         | 800         | 1500        | 40.39       | 600            |
| ZKm401   | 67 | III-3      | 15.8    | 11        | 8.66            | 165         | 600         | 1050        | 27          | 435            |
| ZKm401   | 68 | III-3      | 17.5    | 14        | 9.33            | 290         | 850         | 1330        | 31.68       | 560            |
| ZKm404   | 69 | III-3      | 13.9    | 9         | 8.07            | 100         | 620         | 950         | 25.6        | 520            |
| ZKm404   | 70 | III-3      | 16.1    | 8         | 6.47            | 130         | 530         | 900         | 23.98       | 400            |
| ZKm504   | 71 | III-3      | 10.5    | 6         | 2.55            | 120         | 480         | 750         | 21.58       | 360            |
| ZKm504   | 72 | III-3      | 12      | 5         | 3.52            | 160         | 470         | 790         | 19.56       | 310            |
| ZKm504   | 73 | III-3      | 15.15   | 12        | 4.49            | 160         | 720         | 1060        | 29.9        | 560            |
| ZKm506   | 74 | III-3      | 19.8    | 12        | 5.1             | 40          | 470         | 950         | 28.62       | 430            |

Note. Columns 4~5 were obtained from the dynamic penetration test (DPT), columns 6~9 were obtained from the pressuremeter test (PMT), and columns 10~11 were engineering parameters derived using equations (3) and (4).

1970s [3]. The DPT apparatus consists of a 120 kg hammer with a free-fall height of 100 cm dropped onto an anvil attached to 60 mm diameter drill rods, which in turn are attached to a solid cone tip with a diameter of 74 mm and a cone angle of 60° (Figure 5) [11]. The blow counts for penetrating every 10 cm of soils are recorded and termed as  $N_{120}$ . The DPT is applicable to gravelly soils and weathered extreme-soft and soft rocks [5]. The DPT is widely used in the geotechnical survey in valleys consisting of deep overburden in southwestern China because

of its characteristics of easy operation, wide applicability to different types of soils, and cheap cost.

It is controversial about whether or not to correct the DPT blow count and how to correct it [5]. Currently, the Chinese Code suggests multiplying a correction factor ( $\alpha$ ) to the raw DPT blow counts following equation (1) to get the corrected DPT blow count ( $N_{120}'$ ). Since DPT was widely used to support the foundation design on gravelly soils located in Chengdu Plain, the Design Code for Building Foundation of Chengdu Region [13], hereinafter called

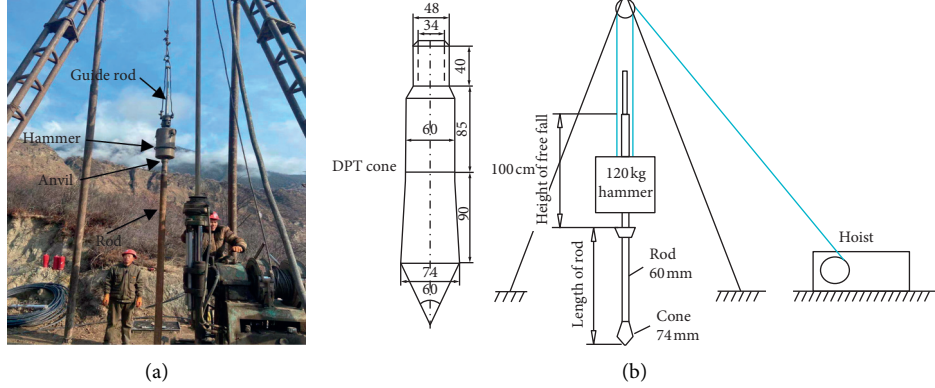


FIGURE 5: (a) Photo of the in situ dynamic penetration test (DPT). (b) Sketch of the DPT apparatus [3].

Chengdu Code, recommends empirical relationships to estimate the soil deformation modulus, compression modulus, and ultimate capacity of gravelly soils using  $N'_{120}$  based on large amount of engineering practices (see Appendix A):

$$N'_{120} = \alpha N_{120}, \quad (1)$$

where  $N'_{120}$  is the corrected DPT blow count,  $N_{120}$  is the raw DPT blow count, and  $\alpha$  is the correction factor that is available for rod length ( $L$ ) less than 19 m and  $N_{120}$  below 40 (see Appendix B).

**3.2. Pressuremeter Test.** The pressuremeter test (PMT) is an in situ test developed by Menard [14] to measure the deformation properties of soil and weak rock. The PMT consists of placing an inflatable cylindrical probe in a pre-drilled borehole and expanding this probe, while measuring the changes in volume and pressure in the probe [15]. The measured volume change of the probe is plotted against the applied pressure (see Figure 6). The pressuremeter modulus is determined as follows [15]:

$$E_{\text{PMT}} = 2 \cdot (1 + \mu) \cdot (V_o + V_m) \cdot \left( \frac{\Delta P}{\Delta V} \right), \quad (2)$$

where  $E_{\text{PMT}}$  is the pressuremeter modulus (MPa),  $p_0$ ,  $p_f$ , and  $p_L$  are initial, yield, and limit pressure, respectively,  $V_0$  is initial volume of the probe ( $\text{cm}^3$ ),  $V_m$  is the corrected volume reading in the center portion of  $\Delta V$  (volume increase),  $\Delta P$  is corrected pressure increase in the center part of the straight line portion of the pressure-volume curve, and  $\mu$  is Poisson's ratio.

It is noted that the PMT measures are associated with the horizontal stresses compared with the vertical resistance measured by the penetration tests (e.g., SPT, CPT, and DPT). Many empirical correlations have been proposed to convert PMT measures to various soil parameters [5, 14] and other penetration test measures [16–23]. The PMT measures are commonly used [5] to calculate the bearing capacity and deformation modulus of foundation soils following equations (3) and (4). The bearing capacity and deformation modulus of soil samples in the compiled dataset are calculated and shown in Table 2:

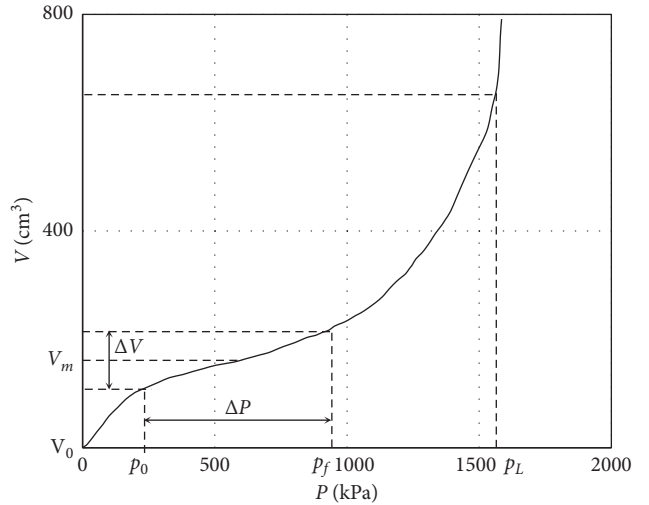


FIGURE 6: Typical graphical form of pressure ( $p$ ) versus total cavity volume change ( $V$ ) from a PMT test.

$$f_{ak} = p_f - p_0, \quad (3)$$

$$E_0 = K \cdot E_{\text{PMT}}, \quad (4)$$

where  $f_{ak}$  is bearing capacity (MPa),  $E_0$  is the deformation modulus (MPa), and  $K$  is the ratio between the deformation modulus and pressuremeter modulus and is dependent on the soil type. The empirical model for cohesive soils (clay, silt, and sand) is used here:  $K = 1 + 61.1m^{-1.5} + 0.0065(V_0 - 167.6)$ , where  $m$  is the ratio between the pressuremeter modulus and the difference of limited pressure and initial pressure, i.e.,  $m = (E_{\text{PMT}}/p_L - p_0)$  [5].

## 4. Results

With the DPT and PMT dataset compiled in Section 3, this section develops the empirical relationships for estimating correction factors (Section 4.1) and soil parameters (Section 4.2) from DPT test results using the regression analysis.

**4.1. Empirical Relationship for DPT Correction Factor.** As mentioned in Section 3, the correction factors of  $N_{120}$  in the Chinese Code are only available for rod length less than 19 m and raw DPT blow counts less than 40. This section aims to extend the correction factors for longer rod lengths (i.e., deeper soils). To achieve this purpose, 11 pairs of data with correction factors suggested by the Chinese Code (see Appendix B) are firstly filtered out to build a regression model between the deformation modulus  $E_0$  and  $N'_{120}$ . These data are from the sublayer III-3, with rod length ranging from 10.5 to 17.5 m. The regression results are shown in equation (5) and Figure 7. The adjusted  $R^2$  of this regression is 0.986, and the  $p$  value of the  $F$ -test and  $t$ -test is 0.000 (less than 0.05), indicating that the regression model is significant and reliable:

$$E_0 = 11.7585 + 2.3674 \times N'_{120}, \quad \text{Adjusted } R^2 = 0.986, \quad (5)$$

where  $E_0$  is the deformation modulus (MPa) and  $N'_{120}$  is the corrected DPT blow count.

Using the reverse form of (5),  $N'_{120}$  for the other 38 data from sublayer III-3 but with rod length exceeding 19 m is calculated in Table 2. Then, its correction factors are calculated as the ratio of  $N'_{120}$  over  $N_{120}$ . Combining the inverted correction factors according to sublayer III-3 soil data and (5), with the correction factors suggested by Chinese Code (See Appendix B), nonlinear regression is undertaken using the Curve Fitting Toolbox of Matlab [24]. The empirical equation for predicting the DPT correction factor using raw DPT blow count and rod length is shown in the following equation:

$$\alpha = 1.021L^{-0.1033}N_{120}^{-0.0356\ln(L)}, \quad \text{Adjusted } R^2 = 0.991, \quad (6)$$

where  $\alpha$  is the DPT correction factor,  $L$  is the rod length (m), and  $N_{120}$  is the raw DPT blow counts.

The 3D visualization of the regression model and the utilized dataset is shown in Figure 8. The relationship between correction factors and rod length for selected  $N_{120}$  values (i.e., 10 to 50 with step of 10) is shown in Figure 9. According to Figure 9, we can see the correction factors decrease with rod length with gradually reducing change rates. The correction factors for higher  $N_{120}$  values decrease faster than the ones for lower  $N_{120}$  values. The DPT correction factors calculated using equation (6) are compared with ones suggested by Chinese Code (Figure 10). The results of the proposed model generally match well with the ones in code, except for very low and high  $N_{120}$  values. The model underestimates the correction factors for  $N_{120}$  of 1, while slightly overestimates the correction factors for  $N_{120}$  of 40 for rod length exceeding 16 m.

**4.2. Empirical Relationships Using Corrected DPT Blow Count.** Empirical relationships are widely used to predict unknown engineering properties of soils [25–27]. In this section, the relationships between the corrected DPT blow counts ( $N'_{120}$ ) and soil parameters derived from

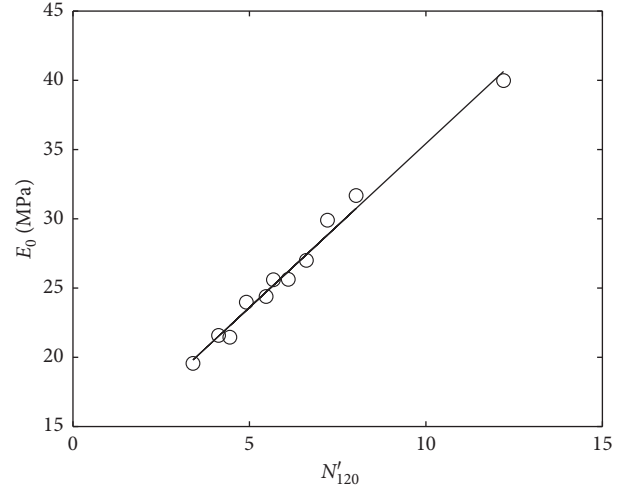


FIGURE 7: Correlation between the deformation modulus and corrected DPT blow counts for shallow soils within sublayer III-3.

pressuremeter measures (i.e., pressuremeter modulus and limit pressure) and engineering parameters used in the foundation design (i.e., soil deformation modulus and bearing capacity) were developed separately. The empirical relationships for engineering parameters are expected to be useful for geotechnical practices in China since soil deformation modulus and bearing capacity parameters are calibrated following the Chinese Codes (see equations (3) and (4)). Linear regression analyses are undertaken using all 74 data pairs belonging to soil Layer III and the reduced number of data pairs belonging to different sublayers of soil Layer III. The best-fit regression equations for soil Layer III (including both sand and clay soils) are shown in equations (7)–(10). The regression coefficients (intercept and slope values for linear regression) and corresponding statistical test results using data from each sublayer and all data from Layer III are summarized in Tables 3–6 and visualized in Figures 11 and 12. The coefficient of determination (adjusted  $R^2$  value) is used to evaluate the goodness of fit of the regression model. The  $F$ -test and  $t$ -test are used to assess the statistical significance of the regression models and the estimated regression coefficients, respectively. Models with larger  $F$ -statistic,  $t$ -statistic, and adjusted  $R^2$  value are better:

$$E_{\text{PMT}} = 3.4437 + 0.5194N'_{120}, \quad \text{adjusted } R^2 = 0.439, \quad (7)$$

$$p_L = 0.4655 + 0.0845N'_{120}, \quad \text{adjusted } R^2 = 0.957, \quad (8)$$

$$E_0 = 11.07 + 2.40N'_{120}, \quad \text{adjusted } R^2 = 0.996, \quad (9)$$

$$f_{ak} = 0.2399 + 0.0305N'_{120}, \quad \text{adjusted } R^2 = 0.775, \quad (10)$$

where  $E_{\text{PMT}}$  is the pressuremeter modulus (MPa) derived using equation (2),  $p_L$  is limit pressure (MPa) measured in the pressuremeter test,  $E_0$  is the deformation modulus (MPa) derived using equation (4),  $f_{ak}$  is bearing capacity (MPa) derived using equation (3), and  $N'_{120}$  is the DPT blow counts corrected using equations (1) and (6).

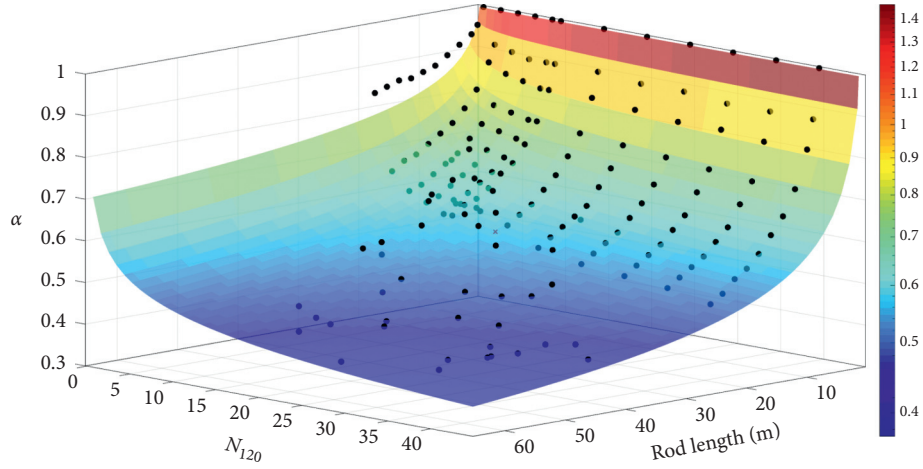
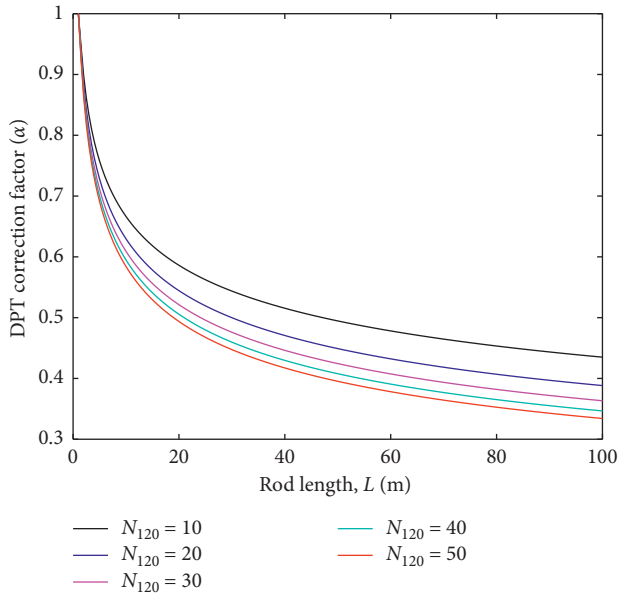
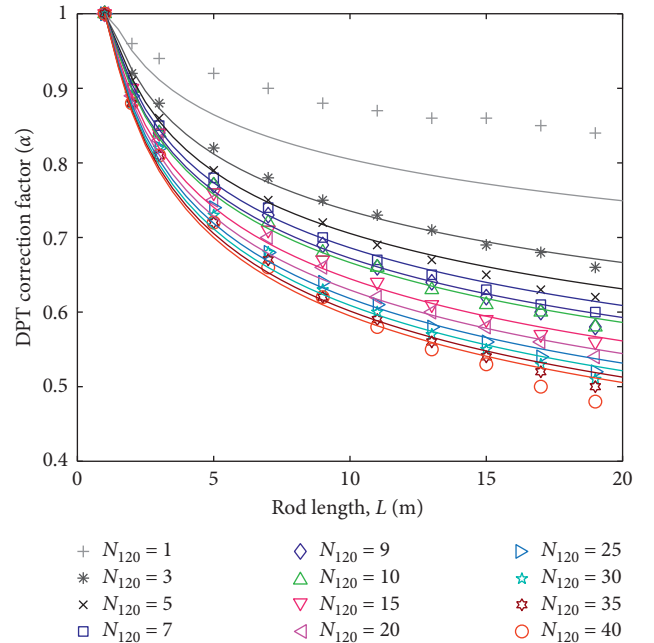


FIGURE 8: 3D visualization of the nonlinear regression model for DPT correction factors.

FIGURE 9: DPT correction factors for the selected N<sub>120</sub> values.

Overall, the regression models using all data (equations (8)–(10)) have adjusted the  $R^2$  value higher than 0.75 except for the regression model for estimating pressuremeter modulus (7). The regression models using all data generally have higher adjusted  $R^2$  than the models using a subset data for different sublayers (see Tables 3–6). In total, 14 of the 16 regression models shown in Tables 3–6 have the  $p$  value for the  $F$ -test and  $t$ -test associated with the slope coefficient less than 0.1, which indicates that the linear regression models and regression coefficients are statistically significant for a 90% confidence level. The other two regression models (models for III-1 and III-2 data in Table 3) have not passed the  $F$ -test and  $t$ -test possibly due to the limited number of

FIGURE 10: Evaluation of DPT correction factors for shallow soils. The scatters are correction factors suggested by the Chinese Code for different N<sub>120</sub> values, and the lines are corresponding predicted correction factors estimated using equation (6).

data used in the regression analyses. Nevertheless, these regression results show that the dynamic penetration tests can be used to provide a preliminary estimation of soil parameters calibrated by more expensive pressuremeter tests. Towards improving the predictive ability and reliability of these empirical relationships, future works can collect more explanatory variables and case data, integrate theoretical/numerical analyses [28, 29], and use more advanced regression algorithms [30, 31].

TABLE 3: Results of regression models correlating corrected DPT blow counts  $N'_{120}$  with pressuremeter modulus  $E_{PMT}$ .

| Soil layer | Sample size | Intercept (std) | Slope (std)     | Adjusted $R^2$ | F-stat | t-stat | p value* |
|------------|-------------|-----------------|-----------------|----------------|--------|--------|----------|
| III        | 74          | 3.4437 (0.7223) | 0.5194 (0.0681) | 0.439          | 58.2   | 7.6282 | 0.000    |
| III-1      | 10          | 10.094 (4.4029) | 0.0985 (0.2675) | -0.106         | 0.136  | 0.3682 | 0.722    |
| III-2      | 15          | 3.9537 (0.7947) | 0.1292 (0.1439) | -0.014         | 0.805  | 0.8974 | 0.386    |
| III-3      | 49          | 4.3713 (1.1086) | 0.4747 (0.1080) | 0.276          | 19.3   | 4.3937 | 0.000    |

\*  $p$  value in italic font indicates that the corresponding regression model is not statistically significant for a  $p$  value of 0.1 (i.e., a 90% confidence level).

TABLE 4: Results of regression models correlating corrected DPT blow counts  $N'_{120}$  with limit pressure  $p_L$ .

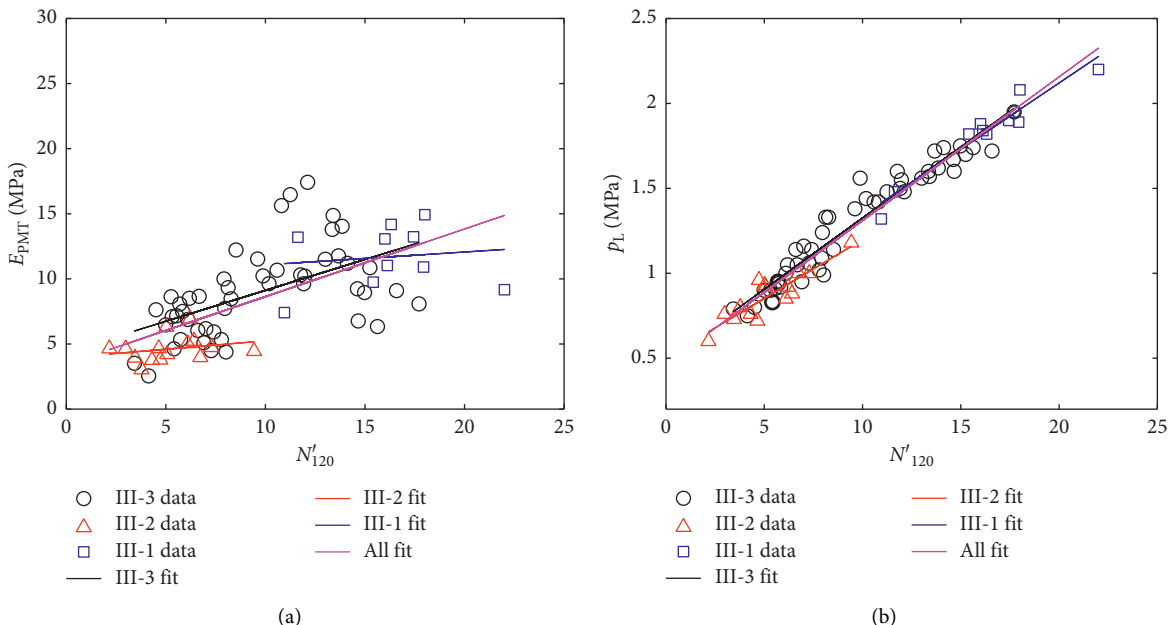
| Soil layer | Sample size | Intercept (std) | Slope (std)     | Adjusted $R^2$ | F-stat | t-stat | p value |
|------------|-------------|-----------------|-----------------|----------------|--------|--------|---------|
| III        | 74          | 0.4655 (0.0222) | 0.0845 (0.0021) | 0.957          | 1630   | 40.392 | 0.000   |
| III-1      | 10          | 0.5619 (0.1263) | 0.0779 (0.0077) | 0.919          | 103    | 10.16  | 0.000   |
| III-2      | 15          | 0.5059 (0.0532) | 0.0692 (0.0096) | 0.783          | 51.6   | 7.18   | 0.000   |
| III-3      | 49          | 0.4869 (0.0330) | 0.0838 (0.0032) | 0.934          | 678    | 26.034 | 0.000   |

TABLE 5: Results of regression models correlating corrected DPT blow counts  $N'_{120}$  with soil deformation modulus  $E_0$ .

| Soil layer | Sample size | Intercept (std) | Slope (std)     | Adjusted $R^2$ | F-stat | t-stat | p value |
|------------|-------------|-----------------|-----------------|----------------|--------|--------|---------|
| III        | 74          | 11.07 (0.1913)  | 2.4015 (0.0180) | 0.996          | 17700  | 133.19 | 0.000   |
| III-1      | 10          | 8.6856 (0.4229) | 2.5279 (0.0257) | 0.999          | 9680   | 98.395 | 0.000   |
| III-2      | 15          | 10.361 (0.2748) | 2.3912 (0.0498) | 0.994          | 2310   | 48.046 | 0.000   |
| III-3      | 49          | 11.891 (0.2306) | 2.3472 (0.0225) | 0.996          | 1090   | 104.47 | 0.000   |

TABLE 6: Results of regression models correlating corrected DPT blow counts  $N'_{120}$  with soil bearing capacity  $f_{ak}$ .

| Soil layer | Sample size | Intercept (std) | Slope (std)     | Adjusted $R^2$ | F-stat | t-stat | p value |
|------------|-------------|-----------------|-----------------|----------------|--------|--------|---------|
| III        | 74          | 0.2399 (0.0204) | 0.0305 (0.0019) | 0.775          | 252    | 15.883 | 0.000   |
| III-1      | 10          | 0.3511 (0.2051) | 0.0232 (0.0125) | 0.216          | 3.47   | 1.864  | 0.099   |
| III-2      | 15          | 0.2408 (0.0222) | 0.0238 (0.0040) | 0.708          | 34.9   | 5.911  | 0.000   |
| III-3      | 49          | 0.2626 (0.0288) | 0.0294 (0.0028) | 0.693          | 109    | 10.461 | 0.000   |

FIGURE 11: Correlations between corrected DPT blow counts  $N'_{120}$ , pressuremeter modulus  $E_{PMT}$ , and limit pressure  $p_L$  for different soil sublayers.

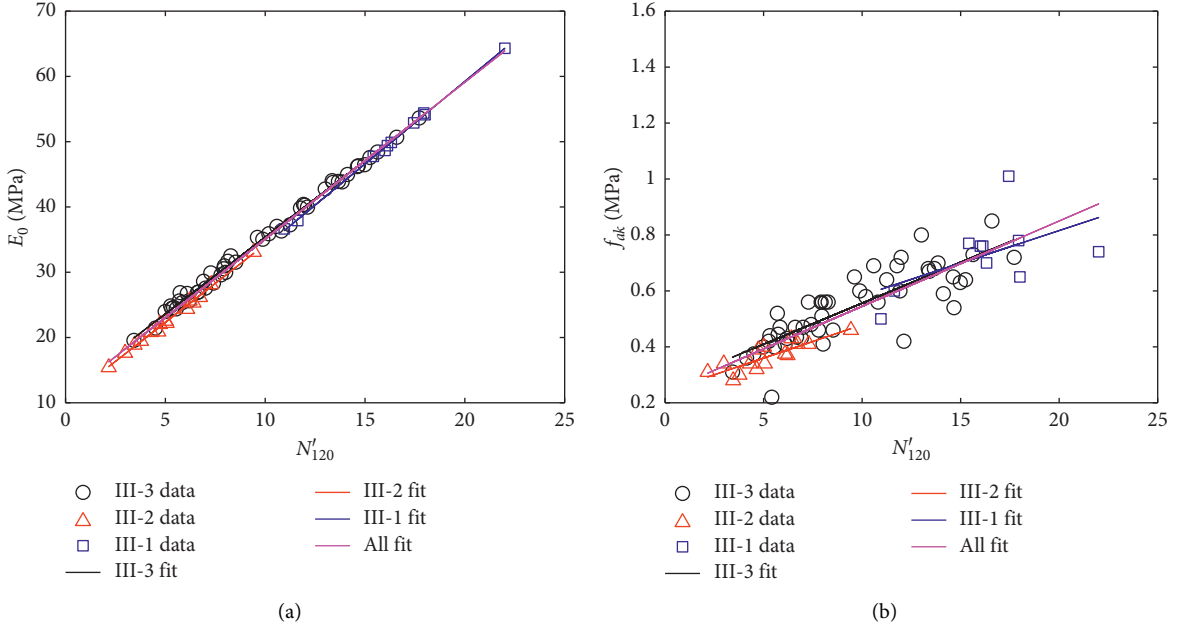


FIGURE 12: Correlations between corrected DPT blow counts  $N_{120}'$ , soil deformation modulus  $E_0$ , and bearing capacity  $f_{ak}$  for different soil sublayers.

TABLE 7: Relationship between ultimate bearing capacity and correct DPT blow counts for gravelly soils in Chengdu Plain (from Chengdu Code DB51/T 5026-2001).

| $N_{120}'$     | 4   | 5   | 6    | 7    | 8    | 9    | 10   | 12   | 14   | 16   | 18   | 20   |
|----------------|-----|-----|------|------|------|------|------|------|------|------|------|------|
| $f_{uk}$ (kPa) | 700 | 860 | 1000 | 1160 | 1340 | 1500 | 1640 | 1800 | 1950 | 2040 | 2140 | 2200 |

TABLE 8: Correction factors for DPT blow counts ( $N_{120}$ ) in the Chinese Code (GB50021-2001).

| Rod length, $L$ (m) | Measured blow count, $N_{120}$ |      |      |      |      |      |      |      |      |      |      |      |
|---------------------|--------------------------------|------|------|------|------|------|------|------|------|------|------|------|
|                     | 1                              | 3    | 5    | 7    | 9    | 10   | 15   | 20   | 25   | 30   | 35   | 40   |
| 1                   | 1                              | 1    | 1    | 1    | 1    | 1    | 1    | 1    | 1    | 1    | 1    | 1    |
| 2                   | 0.96                           | 0.92 | 0.91 | 0.9  | 0.9  | 0.9  | 0.9  | 0.89 | 0.89 | 0.88 | 0.88 | 0.88 |
| 3                   | 0.94                           | 0.88 | 0.86 | 0.85 | 0.84 | 0.84 | 0.84 | 0.83 | 0.82 | 0.82 | 0.81 | 0.81 |
| 5                   | 0.92                           | 0.82 | 0.79 | 0.78 | 0.77 | 0.77 | 0.76 | 0.75 | 0.74 | 0.73 | 0.72 | 0.72 |
| 7                   | 0.9                            | 0.78 | 0.75 | 0.74 | 0.73 | 0.72 | 0.71 | 0.7  | 0.68 | 0.68 | 0.67 | 0.66 |
| 9                   | 0.88                           | 0.75 | 0.72 | 0.7  | 0.69 | 0.68 | 0.67 | 0.66 | 0.64 | 0.63 | 0.62 | 0.62 |
| 11                  | 0.87                           | 0.73 | 0.69 | 0.67 | 0.66 | 0.66 | 0.64 | 0.62 | 0.61 | 0.6  | 0.59 | 0.58 |
| 13                  | 0.86                           | 0.71 | 0.67 | 0.65 | 0.64 | 0.63 | 0.61 | 0.6  | 0.58 | 0.57 | 0.56 | 0.55 |
| 15                  | 0.86                           | 0.69 | 0.65 | 0.63 | 0.62 | 0.61 | 0.59 | 0.58 | 0.56 | 0.55 | 0.54 | 0.53 |
| 17                  | 0.85                           | 0.68 | 0.63 | 0.61 | 0.6  | 0.6  | 0.57 | 0.56 | 0.54 | 0.53 | 0.52 | 0.5  |
| 19                  | 0.84                           | 0.66 | 0.62 | 0.6  | 0.58 | 0.58 | 0.56 | 0.54 | 0.52 | 0.51 | 0.5  | 0.48 |

## **5. Conclusions**

The dynamic penetration test (DPT) has been increasingly used in the geotechnical survey of deep soils in western China. However, the correction factors and empirical relationships for estimating engineering parameters using dynamic penetration test blow counts are still limited to gravelly soils with depth less than 20 m. This work collects 74 DPT measures at a valley site in southwestern China that consists of more than 500-meter-thick overburden soils. A nonlinear empirical relationship dependent on the raw DPT

blow counts and rod length is developed to predict the DPT correction factors for shallow and deep soils through analyzing the deep soil data collected in this work and the existing correction factors for the shallow soils suggested by Chinese Code. Then, the corrected DPT blow counts are used to predict pressuremeter modulus, limit pressure, soil deformation modulus, and bearing capacity derived from more expensive and accurate pressuremeter tests. The results suggest that the proposed empirical relationships are significant and reliable for the investigated deep clay and sand soils. Further studies will be needed to explore the

applicability of the proposed relationships to other soil types and other regions.

## Appendix

### A. Empirical Relationships Using the DPT Blow Counts

Based on many engineering practices, the Chengdu Code provides several empirical relationships to use the corrected DPT blow counts to estimate the deformation modulus, compression modulus, and ultimate bearing capacity of gravelly soils in Chengdu Plain [5, 13].

- (1) Through comparing analysis of DPT and plate load test (PLR) for gravelly soils in Chengdu Plain, the Chengdu Code suggests the use of equation (A.1) to estimate the deformation modulus  $E_0$  (MPa):

$$E_0 = 15 + 2.7N_{120}' \quad (\text{A.1})$$

- (2) Based on the inverse analysis of settlement data of the high-rise building in the Chengdu Plain, the following equation is used to predict the compression modulus  $E_s$  (MPa):

$$E_s = 6.2 + 5.9N_{120}' \quad (\text{A.2})$$

- (3) Table 7 is recommended to estimate the ultimate bearing capacity  $f_{uk}$  (kPa)

### B. Correction Factors for DPT Blow Counts in the Chinese Code

The following table is given in Appendix B of Chinese Code (GB50021-2001) (Table 8).

## Data Availability

The data used to support the findings of this study are available from the corresponding author upon request.

## Conflicts of Interest

The authors declare that they have no conflicts of interest.

## References

- [1] J. K. Mitchell and K. Soga, *Fundamentals of Soil Behavior*, John Wiley & Sons, New York, NY, USA, 2005.
- [2] C. P. Wroth, "The interpretation of in situ soil tests," *Géotechnique*, vol. 34, no. 4, pp. 449–489, 1984.
- [3] Z. Cao, T. L. Youd, and X. Yuan, "Chinese dynamic penetration test for liquefaction evaluation in gravelly soils," *Journal of Geotechnical and Geoenvironmental Engineering*, vol. 139, no. 8, pp. 1320–1333, 2013.
- [4] K. M. Rollins, S. Amoroso, G. Milana et al., "Gravel liquefaction assessment using the dynamic cone penetration test based on field performance from the 1976 Friuli earthquake," *Journal of Geotechnical and Geoenvironmental Engineering*, vol. 146, no. 6, 2020.
- [5] S. Chang and S. Zhang, *Engineering Geology Manual*, China Architecture & Building Press, Beijing, China, 2007, in Chinese, 4th edition.
- [6] R. B. Sancio and J. D. Bray, "An assessment of the effect of rod length on SPT energy calculations based on measured field data," *Geotechnical Testing Journal*, vol. 28, no. 1, pp. 22–30, 2005.
- [7] H. J. Gibbs, "Research on determining the density of sands by spoon penetration testing," *Earth Laboratory Report No. EM-460, United States*, Bureau of Reclamation, 1956, <https://hdl.handle.net/11681/22637>.
- [8] G. T. Housby and R. Hitchman, "Calibration chamber tests of a cone penetrometer in sand," *Géotechnique*, vol. 38, no. 1, pp. 39–44, 1988.
- [9] Y. Zuo and N. Zhao N, "Model tests on modified coefficient of heavy dynamic penetration rod length," *Chinese Journal of Geotechnical Engineering*, vol. 38, no. S2, pp. 178–183, 2016.
- [10] H. Li, F. Guo, S. Fu et al., "Adaptation and correction of dynamic penetration rod length," *Earth Science*, vol. 41, no. 7, pp. 1249–1258, 2018.
- [11] The Ministry of Housing and Urban-Rural Development of China (MOHURD), *Code for Investigation of Geotechnical Engineering*, The Ministry of Housing and Urban-Rural Development of China, Beijing, China, GB 50021-2001, 2001.
- [12] ASTM D2487, *Standard Practice for Classification of Soils for Engineering Purposes (Unified Soil Classification System)*, ASTM International, West Conshohocken, PA, USA, 2017.
- [13] SCCD, *Design Code for Building Foundation of Chengdu Region. DB51/T5026-2001*, Sichuan Province Construction Department (SCCD), 2001, in Chinese.
- [14] L. Menard, "Mesure in situ des propriétés physiques des sols," *Annales des Ponts et Chaussées*, Nabu Press, Paris, France, 1957.
- [15] ASTM D4719, *Standard Test Method for Prebored Pressuremeter Testing in Soils*, ASTM International, West Conshohocken, PA, USA, 2000.
- [16] R. E. Martin, "Estimating foundation settlements in residual soils," *Journal of the Geotechnical Engineering Division*, vol. 103, no. 3, pp. 197–212, 1977.
- [17] S. Ohya S, T. Imai, and M. Matsubara, "Relationships between N value by SPT and LLT pressuremeter results," in *Proceedings of the 2nd European Symposium on penetration testing*, vol. 1, pp. 125–130, Amsterdam, Netherlands, May 1982.
- [18] S. Yagiz, E. Akyol, and G. Sen, "Relationship between the standard penetration test and the pressuremeter test on sandy silty clays: a case study from Denizli," *Bulletin of Engineering Geology and the Environment*, vol. 67, no. 3, pp. 405–410, 2008.
- [19] I. Bozbey and E. Togrol, "Correlation of standard penetration test and pressuremeter data: a case study from Istanbul, Turkey," *Bulletin of Engineering Geology and the Environment*, vol. 69, no. 4, pp. 505–515, 2010.
- [20] A. Kayabasi, "Prediction of pressuremeter modulus and limit pressure of clayey soils by simple and non-linear multiple regression techniques: a case study from Mersin, Turkey," *Environmental Earth Sciences*, vol. 66, no. 8, pp. 2171–2183, 2012.
- [21] J. Monnet, *In Situ Tests in Geotechnical Engineering*, John Wiley & Sons, New York, NY, USA, 2015.
- [22] A. Cheshomi and M. Ghodrati, "Estimating Menard pressuremeter modulus and limit pressure from SPT in silty sand and silty clay soils. a case study in Mashhad, Iran," *Geomechanics and Geoengineering*, vol. 10, no. 3, pp. 194–202, 2015.
- [23] A. Özvan, İ. Akkaya, and M. Tapan, "An approach for determining the relationship between the parameters of

- pressuremeter and SPT in different consistency clays in Eastern Turkey," *Bulletin of Engineering Geology and the Environment*, vol. 77, no. 3, pp. 1145–1154, 2018.
- [24] Matlab, *Matlab R2018b*, The MathWorks Inc., Natick, MA, USA, 2018.
  - [25] I. M. Idriss and R. W. Boulanger, "SPT- and CPT-Based Relationships for the Residual Shear Strength of Liquefied Soils," in *Proceedings of the 4th International Conference on Earthquake Geotechnical Engineering*, pp. 1–22, Thessaloniki, Greece, June 2007.
  - [26] H. Bolton Seed, K. Tokimatsu, L. F. Harder, and R. M. Chung, "Influence of SPT procedures in soil liquefaction resistance evaluations," *Journal of Geotechnical Engineering*, vol. 111, no. 12, pp. 1425–1445, 1985.
  - [27] İ. Akkaya, A. Özvan, and E. E. Özvan, "A new empirical correlation between pressuremeter modules ( $E_m$ ) and shear wave velocity ( $V_s$ ) for clay soils," *Journal of Applied Geophysics*, vol. 171, Article ID 103865, 2019.
  - [28] E. Conte, R. M. Cosentini, and A. Troncone, "Shear and dilatational wave velocities for unsaturated soils," *Soil Dynamics and Earthquake Engineering*, vol. 29, no. 6, pp. 946–952, 2009.
  - [29] E. Conte, L. Pugliese, and A. Troncone, "Post-failure analysis of the Maierato landslide using the material point method," *Engineering Geology*, vol. 277, Article ID 105788, 2020.
  - [30] R. Z. Moayed, A. Kordnaej, and H. Mola-Abasi, "Pressuremeter modulus and limit pressure of clayey soils using GMDH-type neural network and genetic algorithms," *Geotechnical & Geological Engineering*, vol. 36, no. 1, pp. 65–178, 2018.
  - [31] M. Wu, S. S. C. Congress, L. Liu, G. Cai, W. Duan, and R. Chen, "Prediction of limit pressure and pressuremeter modulus using artificial neural network analysis based on CPTU data," *Arabian Journal of Geosciences*, vol. 14, no. 1, pp. 1–18, 2021.